Mechatronics and Automation Technology
J.-Y. Xu (Ed.)

doi:10.3233/ATDE231094

Dynamic Modeling and Cushioning Performance Optimization of Double-Rod Viscoelastic Damper

Shuo WANG[a,1], Guopeng JIA[a], Tenghui WANG[b], Jialiang ZHOU[a] and Junzhou HUO[a]
[a] *Dalian University of Technology, Liaoning 116024, China*
[b] *Beijing Institute of Mechanical Equipment, Beijing 100076, China*

Abstract. Dynamic modeling and cushioning performance analysis are the basis for damper design. The present aims to provide a dynamic model and optimization method for viscoelastic damper. For this purpose, a new double-rod viscoelastic damper for high-speed impact is taken as an example to demonstrate the design process. Firstly, the structure of double-rod viscoelastic damper is described to reveal its working principle. According to the properties of mastic material, a Kelvin model with variable stiffness is established by Simulink. Secondly, the influence of key component parameters on cushioning performance was analyzed for further optimization. Thirdly, based on Simulated Annealing algorithm, the viscoelastic damper system's left piston rod diameter, piston thickness and inner cylinder diameter are chosen as the optimization variables. The optimized viscoelastic damper's peak cushioning force is 31% lower and its cushioning effectiveness is 28% higher. The numerical results provide theoretical recommendations for the double-rod viscoelastic damper design.

Keywords. Double-rod viscoelastic damper, dynamic model, Simulink, simulated annealing algorithm.

1. Introduction

With the goal to efficiently reduce the vibration or impact of mechanical devices, dampers have been recommended as a safety device that converts the kinetic energy of impact into thermal energy dissipation or elastic energy absorption. It is extensively employed in many domains, including automobile traffic, military and industrial production[1-2]. The structural parameters have a direct impact on a damper's ability to provide cushioning, and unreasonably designed structural characteristics can result in varying degrees of damper failure. For instance, in the Luoyang sector, 220 QKX100 viscoelastic dampers were discovered to be leaking as a result of high impact force in just three years [3]. As a result, it's essential to create a mathematical model of damper characteristics, and make targeted adjustments to the damper structure parameters.

Lewandowski[4] took into account the influence of temperature on the dynamic characteristics of systems with VE dampers. Lim[5] built a collision model for rubber and hydraulic coupling buffer system, and analyzed the buffer force by dividing it into damping force and friction force. Bratu[6] solved the problem of dynamic stiffness of

[1] Corresponding Author, Shuo WANG, Dalian University of Technology, School of Mechanical Engineering, Dalian, China; Email: ws18437905878@163.com.

structural system under forced vibration by means of natural elastic characteristics, mass and viscous damping coefficient. Shen[7] analyzed the effects of different fluid viscous damper parameters on seismic performance. Based on the flow continuity equation, Jia and Wang[8-9] developed a mathematical model of the oil buffer, and used genetic algorithms and simulated annealing algorithms respectively to optimize the position and size of the damping hole. By creating a kinetic model of the viscoelastic counter-recoil device, An[10] modified structural parameters to achieve various cushioning properties. Hao[11] built a dynamic model of the artillery's hydraulic buffer, and modified the throttle rod profile curve based on the MATLAB simulation.

For the new type of double-rod viscoelastic damper, this paper starts by describing the structure and working principle. Then a Kelvin model with variable stiffness is established by Simulink. Finally, based on SA algorithm, the structural parameters of viscoelastic damper is optimized to improve the cushioning performance.

2. Dynamic Modeling of New Double-rod Viscoelastic Damper

2.1. Double-rod Viscoelastic Damper Structure

Figure 1 depicts a new design of compact double-rod viscoelastic damper, which is mainly installed on a certain type of firing device. The damper is made up of the components: a cylinder, piston rod, impactor, two covers, flange, guide sleeve, and seal. Elastomer is put into the chamber.

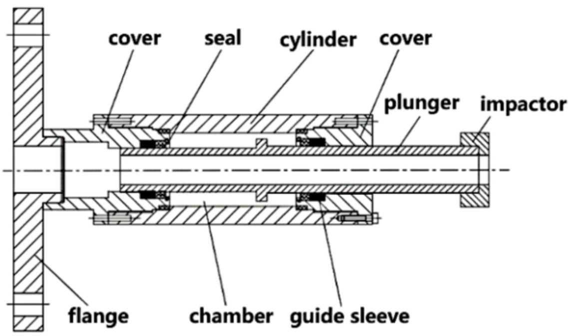

Figure 1. Schematic diagram of the structure of viscoelastic damper

The piston and piston rod are merged to bear more impact and boost the damper's capacity. Right piston rod diameter is greater than left rod diameter on both sides of the piston. When the external force strikes the impact head of the damper, the piston and right piston rod are driven into the cylinder and the left piston rod extends the cover. The volume of elastomer is compressed as a result of the piston rod's different cross-sectional area, which creates a response force on the piston and converts the kinetic energy from the external impact into elastic potential energy. When the impactor speed is 0, the compressed elastomer volume will naturally expand, and the piston rod will spring back to its initial position. Basic parameters of viscoelastic damper are shown in table 1.

Table 1. Basic parameters of double-rod viscoelastic damper

Type	Physical quantity	Column
Density	$\rho / kg \cdot m^{-3}$	980
Consistency factor	μ	2000
Flow index	n	0.45
Inner diameter of cylinder	D/mm	50
Piston diameter	D_0/mm	46
Left diameter of piston rod	d/mm	28
Right diameter of piston rod	d_1/mm	32
Inner diameter of piston rod	d_0/mm	20
Thickness of piston	l/mm	15

2.2. Dynamic Modeling of Damper

An organosilicon polymer mixture between a solid and a liquid makes up the elastomer medium inside the damper, and the viscoelasticity of the elastomer made from various elastomeric materials varies. It is known that the viscoelastic damper has both viscous dissipative and elastic energy storage properties [12]. The dynamic model of viscoelastic damper can be equivalently analyzed using the fractional Kelvin model with variable stiffness. The model is shown in figure 2, consisting of a variable stiffness spring element, a viscous element, and a Scott-Blair element[13]. The mechanical equations of the model can be expressed as

$$\begin{cases} (M+m)\ddot{x} = -(Kx^{\beta} + J(\dot{x})^{\alpha} + C), & v \geq 0 \\ (M+m)\ddot{x} = Kx^{\beta} + J(\dot{x})^{\alpha} - C, & v < 0 \end{cases} \tag{1}$$

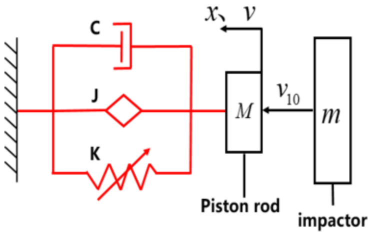

Figure 2. Dynamic model of viscoelastic damper

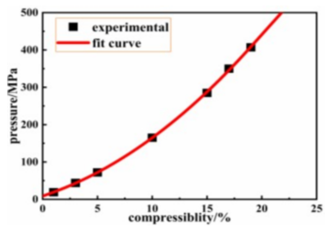

Figure 3. Fitting relation between of elastomer

Where Kx^{β} is the elastic force of spring element; $J(\dot{x})^{\alpha}$ is the viscous damping force of Scott-Blair element; C is friction force of viscous element.

- Elastic force F_K

The pressure of elastomer will change with compression rate. According to the structure of viscoelastic damper, the expression for compression ratio δ can be written as

$$\delta = \frac{S_{left} - S_{right}}{V} x \tag{2}$$

Where x is the displacement of piston movement; V is the volume of elastomer in the damper; S_{left} and S_{right} are the left and right piston area, which can be written as

$$\left(S_{left}, S_{right}\right) = (\pi\left(D_0^2 - d^2\right)/4, \pi\left(D_0^2 - d_1^2\right)/4) \tag{3}$$

The pressure change P with can be measured by universal testing machine and volumetric elastic modulus measuring device. The relationship curve is obtained by Matlab fitting as shown in figure 3, and its expression can be written as

$$P_\delta = 0.0006\delta^3 + 0.588\delta^2 + 9.62\delta + 9.196 \tag{4}$$

The pressure produced by the compression of elastomer acts on the piston face to produce the elastic force, which can be obtained as follows

$$F_K = P_\delta \cdot (S_{left} - S_{right}) = \begin{pmatrix} K_1 & K_2 & K_3 & K_4 \end{pmatrix} (x^{\beta_1} \quad x^{\beta_2} \quad x^{\beta_3} \quad x^{\beta_4})^T \tag{5}$$

where

$$\begin{pmatrix} K \\ \beta \end{pmatrix} = \begin{pmatrix} 0.0006\dfrac{(S_{left} - S_{right})^4}{V^3} & 0.588\dfrac{(S_{left} - S_{right})^3}{V^2} & 9.62\dfrac{(S_{left} - S_{right})^2}{V} & 9.196(S_{left} - S_{right}) \\ 3 & 2 & 1 & 0 \end{pmatrix} \tag{6}$$

- Viscous damping force F_C

The viscous damping force occurs when the elastomer flows through the gap between the piston and the cylinder. The overall flow rate of the elastomer flows through the ring gap can be estimated by utilizing the slit flow characteristics and connected with the power-law fluid's intrinsic shear rate relationship as follows

$$Q = \frac{\pi\left(D + D_0\right)}{4}\left[\frac{n}{(2n+1)}\left(\frac{\Delta p}{2\mu l}\right)^{1/n} h^{(2n+1)/n} + h\dot{x}\right] \tag{7}$$

Considering that the elastomer inside the damper is compressible, the volume of the elastomer in the high-pressure cavity during the buffer time Δt is mainly as follows

1) Volume of elastomer flowing from the annular gap $-Q\Delta t$;
2) Volume of the compressed elastomer $-V\Delta\delta$;

The continuity equation for the buffer chamber flow is

$$A \cdot \Delta x = Q \cdot \Delta t + V\Delta\delta \tag{8}$$

The pressure difference Δp of the elastomer can be written as

$$\Delta p = \frac{2\mu l(2n+1)^n\left[(D^2 - d_1^2) - \left(D + D_0\right)h\right]^n}{n^n h^{(2n+1)}\left(D + D_0\right)^n}(\dot{x})^n \tag{9}$$

Δp acts on the piston to form the damping force F_C, which can be obtained as follows

$$F_C = \Delta p \cdot \frac{\pi\left(D_0^2 - d^2\right)}{4} = \frac{\pi\mu l\left(D^2 - d^2\right)(2n+1)^n\left[\left(D^2 - d_1^2\right) - \left(D + D_0\right)h\right]^n}{2n^n h^{(2n+1)}\left(D + D_0\right)^n}(\dot{x})^n \quad (10)$$

- friction force F_f

Friction force Ff can be obtained from static pressure test. Ff can be written as

$$F_f = C = 275.5N \quad (11)$$

In order to reflect the change of buffering force, nonlinear differential equations are used to represent the dynamics model, which is obtained as

$$\begin{cases} \dfrac{dv}{dt}(m+M) = -F_K - F_C - F_f, \quad v \geq 0 \\ \dfrac{dv}{dt}(m+M) = F_K + F_C - F_f, \quad v < 0 \\ \dfrac{dx}{dt} = v \\ E = \sum\limits_{i=1}^{k}(F_K(i) + F_C(i) + F_f)\cdot(x(i) - x(i-1)), \quad v \geq 0 \end{cases} \quad (12)$$

where E is the cushioning capacity of the viscoelastic damper; $F_K(i)$、$F_C(i)$、$x(i)$ is the elastic recovery force, viscous damping force and displacement at moment i.

The impact process of viscoelastic damper can be reflected in the differential equations mentioned above. Fourth-order Runge-Kutta with a fixed step size is used to apply the model of viscoelastic damper in Simulink and solve the set of state equations of damper. Figure 4 shows the model in detail.

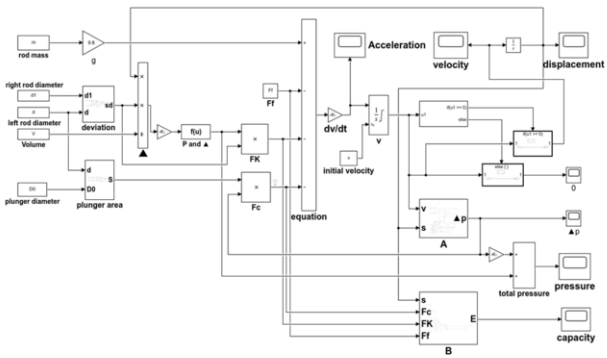

Figure 4. Viscoelastic damper Simulink simulation model

In Subsystem, A equation is the simulation model for Δp calculation; B equation is the simulation model for Equation 4 cushioning energy calculation.

2.3. Influence of Key Component Parameters on Cushioning Performance

According to the dynamic model of the damper, the cushioning performance is related to component structural factors such as the cross-sectional area difference of the piston rod, the gap width, and the thickness of the piston. The effect of cushioning performance can be obtained by changing the structural parameters involved in the model. The results are shown in figure 5 below for the cushioning characteristic curves.

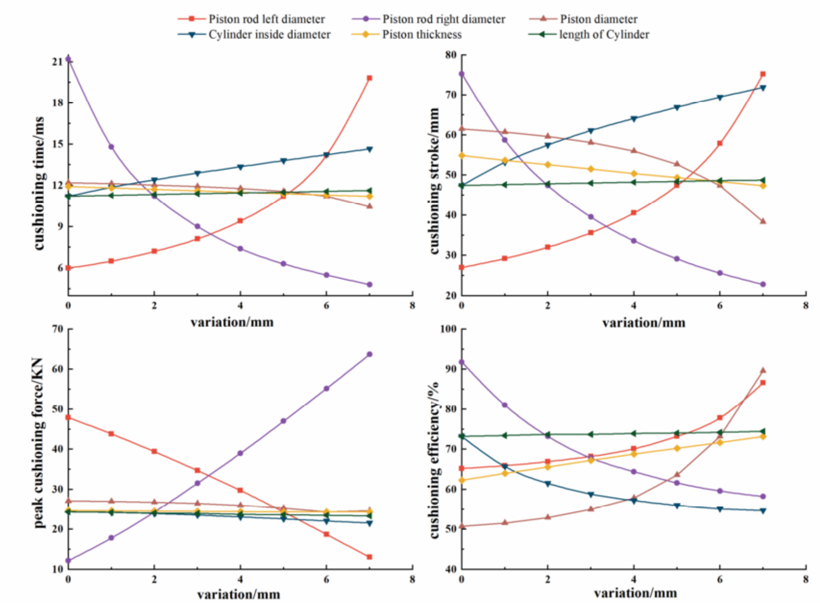

Figure 5. Influence of different parameters on cushioning performance

It can be seen from the figure that the cushioning performance of damper is related to the axial and radial dimensions of cylinder and piston rod. Piston rod parameter design is the most important part of the whole system design. Reasonable design of its structural parameters is the key to improve the performance of viscoelastic damper.

3. Parameter Optimization of Damper Based on SA Algorithm

3.1. SA Algorithm Flow

The process of Simulated Annealing (SA) algorithm is depicted in figure 6 below. Firstly, the initial conditions are established, including the algorithm parameters, objective function, and boundary conditions. Secondly, the initial solution x and objective function $f(x)$ value are calculated. Thirdly, perturbations are generated at random to update to produce a new solution x' and objective function value $f(x')$

under perturbation. When $\Delta = f(x') - f(x) < 0$ is satisfied, the new solution is accepted. Otherwise the new solution is accepted according to the Metropolis criterion. The temperature is lowered continuously until the objective function value are output [14].

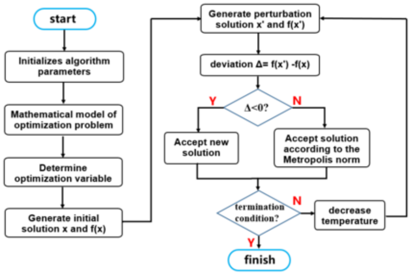

Figure 6. SA optimizes calculation process

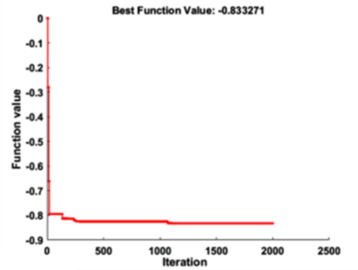

Figure 7. Optimal objective function with iterations

3.2. Optimization Goals

Within the limitations of installation space, damper must have the higher possible cushioning efficiency and the lower peak cushioning force to ensure that it can meet the dependability criteria under high-speed impact situations. While maintaining a consistent cushioning capacity, the viscoelastic damper's cushioning efficiency η and peak cushioning force F_N are multi-objective optimized. η can be written as follows

$$\eta = E / \left(F_N \cdot x_{\max} \right) \tag{13}$$

In multi-objective optimization problems, the linear weighting method is used to obtain the optimization objective function. The target function can be written as

$$\min\{G(Y) = \lambda F_N - \eta\} \tag{14}$$

where λ is the weighting factor.

3.3. Design Variables and Limitations

Three design variables include the left piston rod diameter d, cylinder barrel inner diameter D and piston thickness l. The variable can be written as

$$Y = [d, D, l] \tag{15}$$

Due to the size of the task required, Y is set to ensure a certain structural strength with the following constraints

$$\begin{cases} x_{\max} \le 65mm \\ 20mm < d < 32mm \\ 46mm < D \le 58mm \\ 10mm \le l \le 35mm \end{cases} \quad (16)$$

where $x_{\max}$ is the maximum cushioning displacement.

3.4. Optimization Solution and Results

This paper uses SA optimization module of MATLAB to solve the optimization problems with nonlinear constraints. Figure 7 shows how the ideal objective function changed during the solution process. The objective function reaches convergence accuracy at the 1935th generation and stops annealing at which point the design variables of the viscoelastic damper are $Y = [30.3,\ 48.3,\ 9.6]$. The piston rod's diameter must match the seal of the dynamic seal mechanism, so the diameter of the piston rod's left end is rounded to 30 mm for selection, yielding the damper design variable $Y = [30,\ 48.3,\ 9.6]$.

The structural parameters of viscoelastic damper are substituted into the dynamic model for numerical simulation, and the comparison of cushioning performance curves before and after optimization is shown in figure 8, figure 9 and table 2.

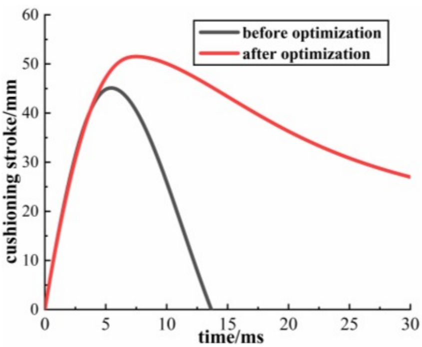

Figure 8. Curve of cushioning stroke and time

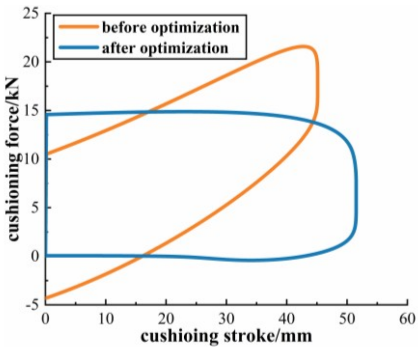

Figure 9. Curve of cushioning force and stroke

Table 2. Cushioning performance before and after optimization

Performance Parameter	Before Optimization	After Optimization	variation
Cushioning time/ms	13.66	394.62	+380.96
Cushioning stroke/mm	45.11	51.51	+6.40
Peak cushioning force/KN	21.59	14.88	-6.71
cushioning efficiency/%	75.81	96.92	+20.62

According to the figure and table, it can be seen that peak cushioning force of the optimized damper decreases significantly, and leads to increase in cushioning stroke and cushioning time. But after optimization, the cushioning stroke is within the rated cushioning stroke of the designed damper, and the cushioning efficiency of the damper is increased by 28% and the peak cushioning force is reduced by 31%. The simulation results can verify the optimization effect. It is conducive to smooth working of the damper and improvement of the service life of mechanical equipment.

4. Conclusion

Based on the new double-rod viscoelastic damper in this paper, the following conclusions can be drawn:

(1) A dynamical model for viscoelastic damper is established to analyze the influence of different structural parameters on the cushioning performance. Simulink platform is designed for simulation and verification.

(2) Based on the SA, peak cushioning force and efficiency of viscoelastic damper are optimized. The results show that the optimized damper's cushioning effectiveness is increased by 28% and the peak cushioning force is decreased by 31%, demonstrating the effectiveness of the optimization.

(3) The results of the simulation provide theoretical recommendations for the double-rod viscoelastic damper design under high-speed impact.

Acknowledgements

This work is supported by the "Unveiling the List and Leading" Major special science and technology project of Liaoning Province(No. 2022JH1/10400031).

References

[1] De Domenico D, Ricciardi G, Takewaki I. Design strategies of viscous dampers for seismic protection of building structures: a review[J]. Soil dynamics and earthquake engineering, 2019, 118: 144-165.
[2] Zhao X, Wei W, Liu S, et al. Dynamic Modeling of Elastic rubber Buffer based on improved PSO Algorithm [J]. Journal of Vibration and Shock, 2020, 39(24): 107-112.
[3] Zhao J. Leakage Cause Analysis and Improvement of Elastic Mud Coupler Buffer for Electric Locomotive [J]. Railway Technical Supervision. 2017, 45(06): 34-37.
[4] Lewandowski R. Influence of Temperature on the Dynamic Characteristics of Structures with Viscoelastic Dampers[J]. Journal of Structural Engineering, 2019, 145(2):04018245.1-04018245.13.
[5] Lim S, Ji Y, Park Y. Simulation of energy absorption performance of the couplers in urban railway vehicles during a heavy collision[J]. Machines. 2021, 9(5): 91.
[6] Bratu P. Dynamic Rigidity of The Linear Voigt-Kelvin Viscoelastic Systems[J]. Romanian Journal of Acoustics and Vibration, 2019, 16(2): 184-188.
[7] Shen D, Kookalani S. Effect of Fluid Viscous Damper parameters on the seismic performance[J]. J Civil Eng Mater, 2020, 4: 141-153.
[8] Jia W. Key Structure Design and Experimental Research of Oil Buffer [D]. Shenyang University of Technology, 2020.
[9] Wang C, Qiu Z, Zeng Q, et al. Optimization of Damping Hole of Porous Hydraulic Buffer Based on Simulated Annealing Algorithm [J]. Chinese Hydraulics & Pneumatics. 2019(04): 54-59.
[10] An X, Gao Y, Zhou J, et al. Mechanical Characteristics Analysis of Elastic Clay Recoil Device [J]. Journal of North University of China (Natural Science Edition). 2022, 43(01): 48-55.
[11] Hao B, Sun W, Pan X. Research on buffering Characteristics of a Hydraulic Buffer of Artillery [J]. Journal of Ordnance Equipment Engineering, 2018, 39(09): 54-58.
[12] Kim H, Yoo W, Ok J, et al. Parameter identification of damping models in multibody dynamic simulation of mechanical systems[J]. Multibody System Dynamics. 2009, 22(4): 383-398.
[13] Karner T, Gotlih J, Razboršek B, et al. Use of single and double fractional Kelvin–Voigt model on viscoelastic elastomer[J]. Smart Materials and Structures, 2019, 29(1): 015006.
[14] Wang C, Wang X, Wei X, et al. Design Optimization and Comparison of Porous Hydraulic Buffer Based on Different Algorithms [J]. Chinese Hydraulics & Pneumatics. 2021(02): 71-76.